

Thermoreversible Gelation of Nitrocellulose Solutions

Ching-Feng Mao, Cheng-Ho Chen

Department of Chemical Engineering, Southern Taiwan University of Technology, Tainan, Taiwan, Republic of China

Received 28 October 2002; accepted 10 May 2003

ABSTRACT: Thermoreversible gelation of concentrated solutions of nitrocellulose was examined. The sol–gel transition diagrams were established using the ball-drop method. The critical gel concentrations (C_{gel}), defined as the lowest concentration for gelation to occur, are approximately proportional to the reciprocal of the molecular weight of nitrocellulose. In addition, the values of $C_{gel}[\eta]$ lie in the concentrated regime where entanglement effects are present. These facts suggest that the entanglement of polymer chains is a necessary condition for the formation of nitrocellulose gels. Moreover, the association of polymer segments is identified as another factor affecting the gel

stability. This is evidenced by both the enhancement of the gel stability in poor solvents and the large enthalpy of mixing at low temperatures. Because of the presence of the association, the number of polymer chains in a junction point is larger than two, which is the value predicted by assuming entanglements as the only factor responsible for gelation. © 2003 Wiley Periodicals, Inc. *J Appl Polym Sci* 90: 4000–4008, 2003

Key words: nitrocellulose; gels; association; gelation; transitions

INTRODUCTION

A thermoreversible polymer gel is a network of polymer chains crosslinked by physical bonds in which solvents are immobilized within. Although there have been many studies of the chain junctions in a physical gel, the nature of these junction points is still a subject of controversy. Several mechanisms of network formation have been proposed to describe the structure of the junctions in a physical network: double- or triple-stranded helical structures, crystallite formation, association of separated polymer chains caused by phase separation, complex formation attributed to solvent–polymer interaction, and molecular entanglements.^{1–3} Although the type of joints can be determined roughly for a particular physical gel system, the details of the network structure remain a matter of debate.

Being one of the widely used cellulose derivatives, nitrocellulose can form thermoreversible gels in a variety of solvents.^{4–7} It is well known that nitrocellulose forms a reversely thermoreversible gel in a poor solvent, which is attributed to the onset of phase separation when the temperature increases.⁴ However, gelation also occurs in a good solvent at high nitrocellu-

lose concentrations,^{6,7} in which the mechanism has not been clearly elucidated.

Several studies concerning the gelation of nitrocellulose have been reported, although their results are controversial. Aggregates or gel-like materials of nitrocellulose in good solvents, such as esters, were reported.^{8,9} These gel particles are attributed to the residue of unreacted cellulose, where the interchain hydrogen bonds of hydroxyl groups resulting from incomplete nitration serve as the crosslinks of microgels. Although this model is quite similar to the helical structures responsible for the network formation of polysaccharide gels in aqueous solutions, macroscopic gelation associated with these aggregates has never been reported. On the other hand, Ninomiya and Ferry¹⁰ attributed the dynamic mechanical behavior of gels of nitrocellulose in diethyl phthalate to the presence of nitrocellulose crystallites. A recent study¹¹ showed that cellulose esters with a low degree of substitution suspended in water consist of crystallites of helically twisted rods. However, there is no direct evidence that nitrocellulose gelation arises from crystallite formation. The gel structure of nitrocellulose gels is still poorly understood. Further study is required to understand the gelation mechanism and the junction structure of a nitrocellulose gel.

In this investigation, we examined the thermoreversible gelation of nitrocellulose in a variety of solvents and established the sol–gel transition diagrams using the ball-drop method. Specifically, we focused on the gel prepared from nitrocellulose in ethyl acetate, which shows typical gelation behavior of nitrocellulose. We also measured the temperature and

Correspondence to: C.-F. Mao (cfmao@mail.stut.edu.tw).

Contract grant sponsor: National Science Council of the Republic of China; contract grant number: NSC 89-2216-E-218-003.

TABLE I
Values of $[\eta]$, C_{gel} , and ΔH_x for Nitrocellulose
in Ethyl Acetate

Sample	\bar{M}_w	$[\eta]^a$ (dL/g)	C_{gel} [η]	ΔH_x (kJ/mol)	n
NC1	1.04×10^5	1.76	31	8.9	2.3
NC2	8.0×10^4	1.35	25	11.9	1.9
NC3	6.4×10^4	1.09	21	7.9	2.4
NC4	4.0×10^4	0.67	23	5.8	2.9
NC5	2.1×10^4	0.35	23	4.8	3.3

^a In ethyl acetate at 303 K.

concentration dependencies of the Flory–Huggins interaction parameter χ for nitrocellulose in ethyl acetate. An interpretation of the gelation behavior based on the thermodynamic analysis follows.

EXPERIMENTAL

Materials

Samples of nitrocellulose [degree of nitration ~ 2.26 (12.0% N)] were kindly provided by T.N.C. Industrial Co. (Taiwan). The corresponding molar mass of the monomer was estimated to be 264. All samples were pretreated to remove residual isopropanol in a vacuum oven at 343 K for 2 h and stored in a desiccator before use. The molecular weights of the polymers were determined from intrinsic viscosity $[\eta]$ in acetone. The weight-average molecular weight (\bar{M}_w) was obtained using values of 1.69×10^{-3} mL/g and 1.0 for K and a in the Mark–Houwink equation¹²:

$$[\eta] = K\bar{M}_w^a \quad (1)$$

The molecular weights of the nitrocellulose samples are summarized in Table I. Solvents were reagent grade and used without further purification.

Nitrocellulose gels (concentration 200–900 g/L) were prepared by dispersing the dried nitrocellulose in a specific solvent at room temperature in a sealed tube.

Gel melting point measurements

The gel melting point was determined using the ball-drop method. A steel ball with a diameter of 5 mm was placed on top of the gel, which was initially immersed in a dry ice/acetone bath at about 210 K. The temperature of the bath was then allowed to increase at a rate of about 1 K/min. The temperature at which the steel ball started to drop was recorded as the gel melting point.

Vapor pressure measurements

The vapor pressure measurements were performed on a homemade apparatus attached to a vacuum pump with an ultimate pressure of 10^{-3} Torr. The apparatus consists of a Pyrex glass cell and a digital vacuum gauge (PSI-Tronix, model PG5000). The glass joint was made of Kimax joints with an O-ring lubricated with vacuum grease, whereas the stainless steel part was connected by Hoke Gyrolok fittings. To test the vacuum system, the vacuum line was disconnected after the apparatus was evacuated, and no leakage was detected in 1 week.

After the sample was placed in the cell, the freezing and melting cycles suggested by Nunes et al.¹³ were conducted to ensure complete degassing of the sample until a constant vapor pressure was established. The cell was then immersed in a temperature bath to establish equilibrium. The equilibrium vapor pressure of the solvent in a gel was recorded as a function of temperature and volume fraction of polymer. The interaction parameter χ was estimated from the equilibrium vapor pressure of the solvent above the gel (p_1) to that above the pure solvent (p_1^0) according to the Flory–Huggins treatment

$$\ln \frac{p_1}{p_1^0} = \ln(1 - \phi_2) + \phi_2 + \chi\phi_2^2 \quad (2)$$

where ϕ_2 is the volume fraction of polymer.

RESULTS AND DISCUSSION

General features of gels

Nitrocellulose dissolved easily in a variety of moderately hydrogen bonding solvents, as shown in Table II. It did not dissolve in poorly or strongly hydrogen bonding solvents, such as toluene or isopropanol. Lowering the temperature of the solution yielded a

TABLE II
Gel Properties of Sample NC3 in Various Solvents

Solvent	Solubility parameter δ (cal/cm ³) ^{1/2}	T_m^a (K)	ΔH_x (kJ/mol)
Nitrocellulose	11.5	—	—
<i>n</i> -Amyl acetate	8.5	304	9.1
<i>n</i> -Butyl acetate	8.5	300	5.5
<i>n</i> -Propyl acetate	8.8	297	4.8
Ethyl acetate	9.1	283	7.9
Tetrahydrofuran	9.1	311	2.1
Methyl ethyl ketone	9.3	284	5.9
Acetone	9.9	270	5.8
Dimethylformamide	9.9	258	4.9
Toluene	8.9	insoluble	—
Isopropanol	11.5	insoluble	—

^a Gel melting temperature at a concentration of 400 g/L.

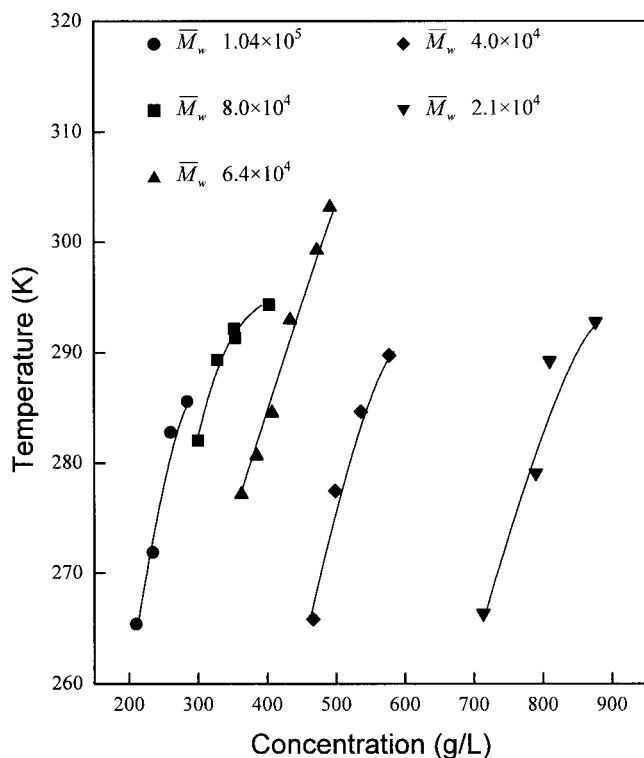


Figure 1 Effect of molecular weight on the gel melting temperature against the concentration of nitrocellulose in ethyl acetate.

transparent gel, indicating that phase separation did not occur during the gelation. These gels were elastic and capable of supporting the steel ball. Typical sol-gel transition phase diagrams for nitrocellulose of various molecular weights in ethyl acetate were obtained using the ball-drop method, as shown in Figure 1. The gel melting point, which represents the gel stability, increased with increasing nitrocellulose concentration. At a given polymer concentration, the gel melting point increased with increasing molecular weight. Some gels were sealed and aged at room temperature for 1 week, and no significant difference in the gel melting points was observed. We also evaluated the effect of heat treatment on the gel behavior, for example, annealing at 323 K for 1 h. Again, the gel melting point was similar to that obtained for the untreated sample. These facts demonstrate that these gels were in a state of equilibrium.

Critical gel concentrations

As indicated in Figure 1, the molecular weight of nitrocellulose strongly affects the gel stability. It is found that, for \bar{M}_w below 2.1×10^4 , gelation was hardly achieved. To elucidate the effect of molecular weight, we measured the critical gel concentration (C_{gel}), defined as the lowest concentration capable of

gelation, as a function of molecular weight, as depicted in Figure 2. The critical concentration was also strongly dependent on the molecular weight of nitrocellulose. The double-logarithmic plot of C_{gel} versus polymer molecular weight leads to a straight line with a slope of -0.91 , showing that a scaling law exists for C_{gel} and the molecular weight (\bar{M}_w).

$$C_{gel} \bar{M}_w^{0.91} = K \quad (3)$$

where K is a constant. The exponent, being approximately unity, is similar to the value derived for the critical condition for the entanglement effect on viscosity behavior in the concentrated regime, which states that the polymer molecular weight is inversely proportional to the critical concentration.¹⁴ Therefore, entanglements are expected to be essential for the formation of these gels.

In addition, through examining the values of $C_{gel}[\eta]$, listed in Table I, entanglements are justified to be a necessary condition for gelation. The product of concentration and intrinsic viscosity, the reduced concentration often used in constructing a master curve of the viscosity for polymer solutions, provides a method for understanding the interaction among polymer chains. In a master curve, two critical concentrations (C^* and C^{**}) can be identified, relating to the overlap concentration and the concentration that polymer chains attain unperturbed dimensions with the onset

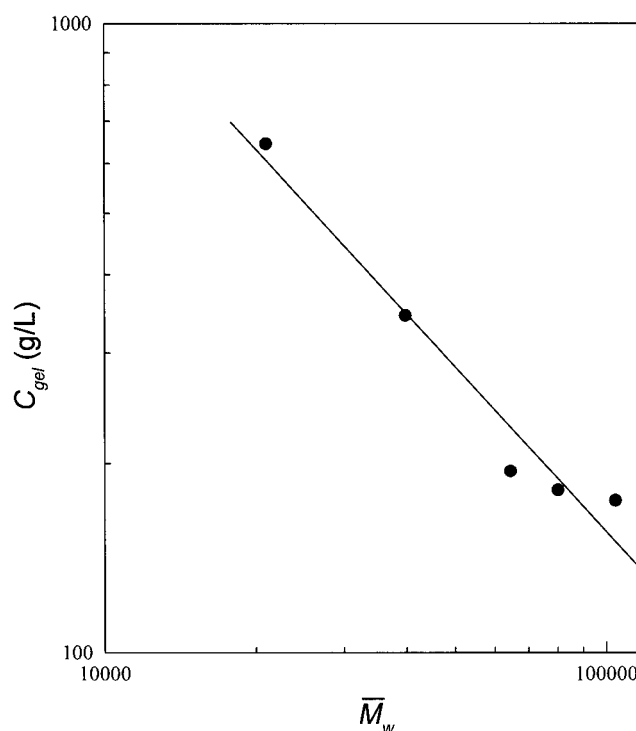


Figure 2 Dependency of the critical gel concentration of nitrocellulose in ethyl acetate on \bar{M}_w .

of chain entanglements, respectively.^{15,16} It has been reported that, for polysaccharides with conformation of random coils, typical values were 0.76 and 3.56 for $C^*[\eta]$ and $C^{**}[\eta]$, respectively¹⁶; however, for a rigid polysaccharide, these values may be higher, depending on the type of polymer and the solvent quality. The values of $C_{gel}[\eta]$ in this study fell within the range from 21 to 31, thus corresponding to the concentrated regime where entanglements are present. Because nitrocellulose is considered as a rigid polymer, even dissolved in a good solvent,¹⁷ its critical concentration for entanglements should be somewhat higher than that for polymers with random coil conformation. Nonetheless, compared to $C^{**}[\eta]$, the values of $C_{gel}[\eta]$ are almost an order of magnitude higher. This difference can be explained by the number density of entanglements required to achieve gelation, which must be higher than that required to cause a change in viscosity increments of the master curve in a viscosity measurement.

Ferry and Eldridge relations

Because these gels are in an equilibrium state, it is reasonable to assume that the equilibrium also exists between actual and potential junctions in the physical networks, and then their sol–gel transition can be represented by the Ferry and Eldridge equations¹⁸

$$\left[\frac{\partial \ln C}{\partial (1/T)} \right]_{\bar{M}_w} = \frac{\Delta H_m}{R(n-1)} = \frac{\Delta H_x}{R} \quad (4)$$

at constant molecular weight \bar{M}_w and

$$\left[\frac{\partial \ln \bar{M}_w}{\partial (1/T)} \right]_C = \frac{\Delta H_m}{R} \quad (5)$$

at constant concentration C . Here, T is the gel melting point in a phase diagram, ΔH_m represents the enthalpy of formation per junction point, and n is the number of polymer chains involved in each junction point. The enthalpy change ΔH_x in eq. (4) corresponds to the addition of one mole of potential junctions to the partially formed network junctions. Equations (4) and (5) imply that linear plots of the logarithm of molecular weight or concentration versus the reciprocal of the gel melting temperature can be obtained if ΔH_m and n are constant.

When the data in Figure 1 were analyzed using eq. (4) for each molecular weight, reasonably linear relationships were obtained, as shown in Figure 3. The corresponding values of ΔH_x are given in Table I. These values are comparable to those for synthetic polymer gels caused by entanglements,^{3,19} but much less than those for nature polymer gels formed because of the entwining of multiple-stranded helix

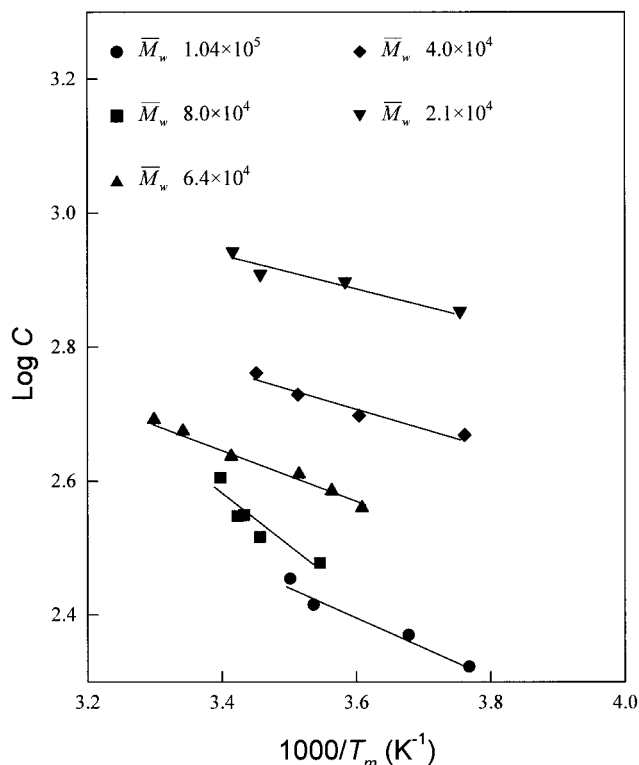


Figure 3 Dependency of $\log C$ on $1/T_m$ for nitrocellulose with various molecular weights in ethyl acetate.

structures.^{18,20} It is noted that the enthalpy change increases with increasing molecular weight. We will return to this point after ΔH_m is calculated using eq. (5).

To evaluate the validity of eq. (5), T_m is expressed as a function of concentration for each \bar{M}_w in Figure 1. Values of T_m at a fixed concentration are then interpolated using this expression. Figure 4 shows the plot of $\log \bar{M}_w$ against the reciprocal of the estimated T_m for nitrocellulose in ethyl acetate at a concentration of 400 g/L. The data remarkably obey the Ferry–Eldridge linear relationship [eq. (5)] with an enthalpy change of $\Delta H_m = 11.2$ kJ/mol. The low value of ΔH_m agrees with the previous finding that entanglements are the crucial elements for the formation of nitrocellulose gels.

Despite the simplified assumptions on which the Ferry–Eldridge relations are based, the enthalpy changes in eqs. (4) and (5) estimated from the sol–gel transition data can provide a picture of the nature of the networks. Comparing the enthalpy changes obtained from eqs. (4) and (5) allows us to determine the value of n for each sample, and these are tabulated in Table I. It is found that the values of n are somewhat higher than 2 for samples with high \bar{M}_w , but they become even much higher at low \bar{M}_w , as graphically shown in Figure 5. If the network junction points are formed by physical entanglements, only two polymer

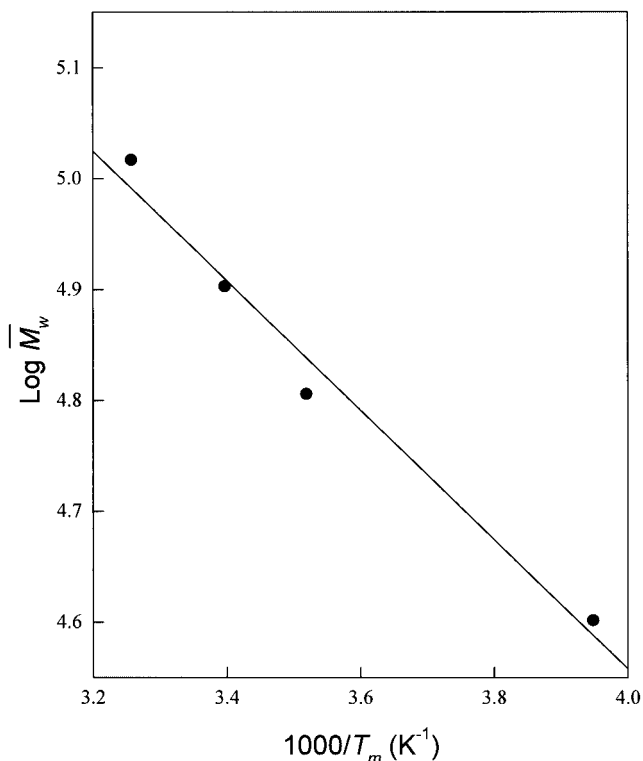


Figure 4 Dependency of $\log \bar{M}_w$ on $1/T_m$ for nitrocellulose in ethyl acetate at a fixed concentration of 400 g/L.

chains are involved in each junction point. Because our values are higher than 2, especially for samples with low \bar{M}_w , there must be factors other than entanglements involved in the formation of networks.

Reports regarding the presence of gel-like aggregates for nitrocellulose in esters^{8,9} provide us a clue for answering this anomaly. Schurz and Tritthart⁹ showed that the gel-like structure for nitrocellulose in esters was branched spherulite and they related it to unreacted cellulose crystallites. Holt et al.⁸ performed light-scattering experiments on nitrocellulose in ethyl acetate, where the downward curvature in the Zimm plot was attributed to the presence of gel-like aggregates. These studies confirm that nitrocellulose can form a microgel phase even in a good solvent, possibly attributable to the unreacted cellulose portion. However, these gel-like aggregates do not lead to gelation on a large scale, given that gelation occurs only in the semidilute regime where the entanglement effect dominates. According to this concept, we speculate that the microgel obtained by aggregation of nitrocellulose can modify the network junctions and insert extra polymer chains in a junction point, thus leading to a value of $n > 2$.

In addition to the aggregation of the heterogeneous portion of nitrocellulose (unreacted cellulose), the association of nitrocellulose segments may also participate in the formation of junction points. We examined

the thermodynamics of nitrocellulose solutions, which is discussed next, showing that the association between polymer segments is favorable under poor thermodynamic conditions. We also performed viscometry and rheometry experiments for nitrocellulose in ethyl acetate in the dilute and semidilute regimes to demonstrate the presence of association and its breakdown with increasing temperature. These results will be presented in a separate study.

Solvent effects

Regarding the effect of solvent on gelation, the gel melting points at a concentration of 400 g/L were selected arbitrarily to represent the gel stability. In Table II the gel melting points and the enthalpy changes ΔH_x are listed together with the solubility parameters of the solvents δ_s . The values of ΔH_x were low regardless of the type of solvents, indicating that no strong interaction exists during the gel melting process, which is consistent with our postulation that the gelation is mainly attributed to entanglements. In a comparison of the gel properties of a series of esters, it was found that the gel melting points increased with increasing molar mass of the solvents, although the enthalpy changes do not show this trend.

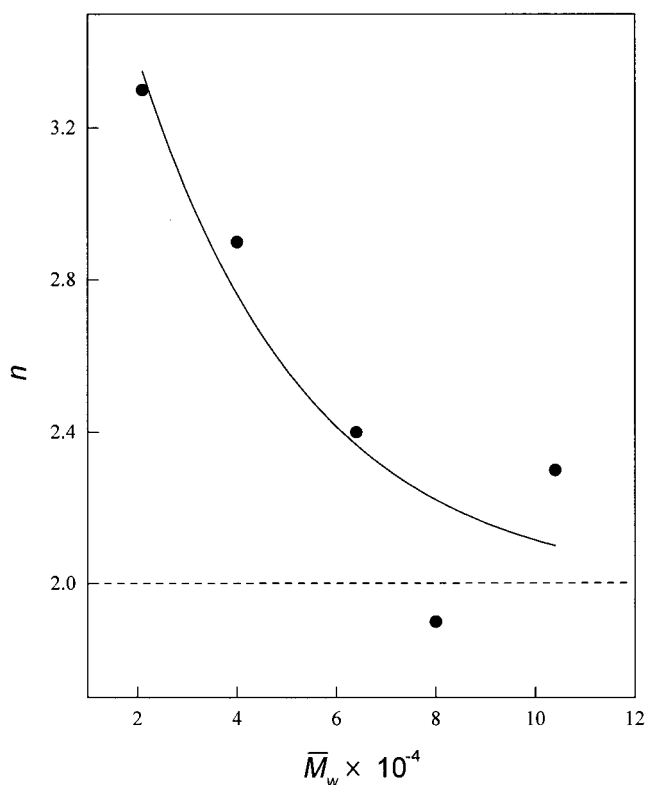


Figure 5 Dependency of the average number of polymer chains in a junction point on \bar{M}_w for nitrocellulose in ethyl acetate (the dashed line represents $n = 2$).

Through examining the effect of solubility parameters on the gel stability for the solvents studied, it was found that the values of T_m decrease with increasing δ_s . It appears that the difference between the solubility parameter of nitrocellulose δ_p , and that of the solvent determines the gel stability. This correlation can be manifested by plotting T_m against $(\delta_p - \delta_s)^2$, as illustrated in Figure 6. The plot yields a linear relationship between $(\delta_p - \delta_s)^2$ and T_m except for the point for nitrocellulose in tetrahydrofuran, which shows considerable deviation. This finding suggests that the gel stability can be enhanced by a poor solvent but reduced by a good solvent. Boyer et al.² reported a similar correlation for atactic polystyrene in a variety of solvents, but they postulated that the gelation behavior is related to overlap of polymer coils by segment-segment interactions instead of entanglements. Here one can rationalize that the disentanglement process during the sol-gel transition depends on the difficulties in breaking the intersegmental contacts, which can be strengthened by a poor solvent, thus leading to greater stability.

Interaction parameters χ and g

The correlation between T_m and $(\delta_p - \delta_s)^2$ (the heat of mixing of polymer solutions) suggests that the gel

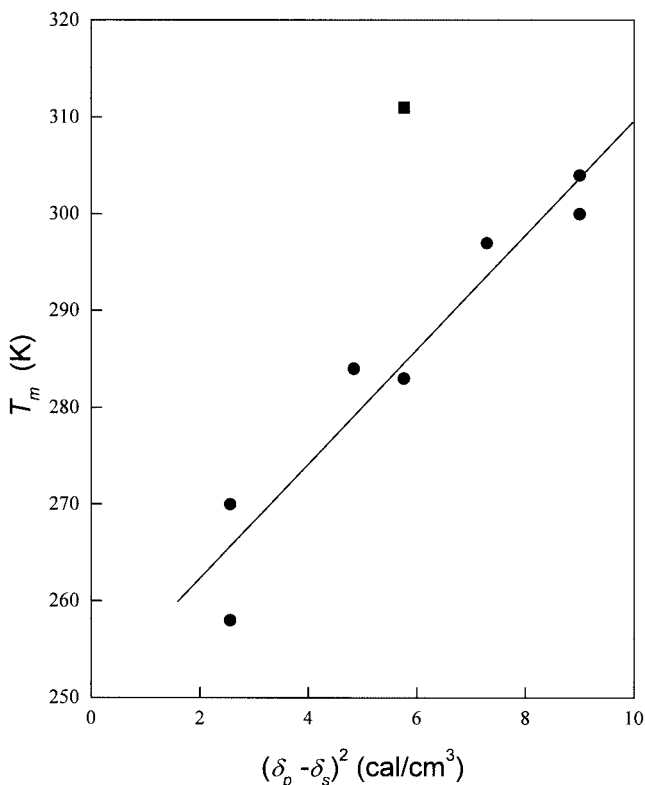


Figure 6 Gel melting temperature as a function of $(\delta_p - \delta_s)^2$ for nitrocellulose in various solvents (■ is the data point for tetrahydrofuran).

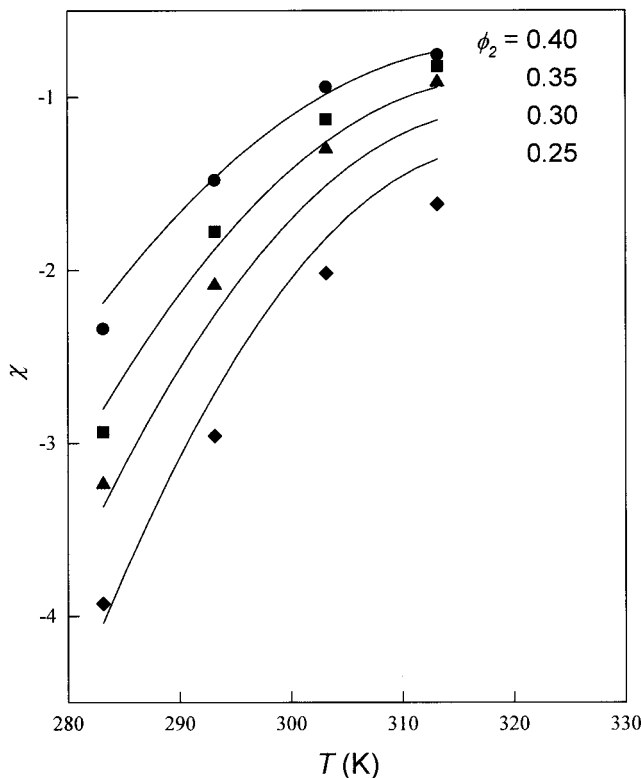


Figure 7 Effect of polymer volume fraction on the χ parameter against temperature for nitrocellulose in ethyl acetate. The curves were obtained by using eq. (9) to fit the experimental data (circles: $\phi_2 = 0.40$; squares: $\phi_2 = 0.35$; triangles: $\phi_2 = 0.30$; diamonds: $\phi_2 = 0.25$).

stability is determined by the thermodynamic states of a polymer solution. However, it is known that $(\delta_p - \delta_s)$ is only a simple measure of solubility, which is not sufficient to determine the Gibbs free energy of mixing and does not account for the variation of temperature and concentration. To describe the thermodynamic states of a polymer solution, one has to measure the temperature and concentration dependencies of the Flory-Huggins interaction parameter χ . Figure 7 shows the variation of the χ parameters for Sample NC3 in ethyl acetate as a function of temperature and volume fraction. It is noted that the χ parameter for this solution is always negative, irrespective of temperature and concentration, and increases with increasing temperature and polymer concentration. Normally negative values of the interaction parameter χ imply good solvency. If this statement is true, our results reveal that ethyl acetate is a good solvent for nitrocellulose and its solvency is enhanced at low temperatures and low polymer concentrations. In comparison with the gelation behavior, the temperature dependency of the χ parameter acts in the opposite direction, which predicts that the formation of gels should occur at high temperatures because of the poor solvency therein. At this point, it seems that the ther-

modynamic data disagree with the observed gelation behavior.

This contradiction is mainly attributed to the fact that the χ parameter corresponds to the partial molar quantities of the solvent rather than the integral ones. The integral interaction parameter g is defined by

$$g \equiv \frac{\Delta G^R}{RTx_1\phi_2} \quad (6)$$

where x_1 is the mole fraction of the solvent and ΔG^R represents the residual molar Gibbs free energy of mixing. With the knowledge of g , the molar Gibbs free energy of mixing for a polymer solution ΔG is then calculated according to

$$\frac{\Delta G}{RT} = x_1 \ln \phi_1 + x_2 \ln \phi_2 + gx_1\phi_2 \quad (7)$$

The χ parameter is related to g by the following formulation²¹:

$$\chi = g - (1 - \phi_2) \frac{\partial g}{\partial \phi_2} \quad (8)$$

When it does not depend on composition, χ is identical to the integral interaction parameter g . With this assumption the aforementioned statement regarding values of χ and solvency is correct. However, Figure 7 shows that χ is highly dependent on composition. Thus, a further analysis based on the integral interaction parameter has to be performed.

To calculate g using eq. (8), the temperature and concentration dependencies of χ have to be evaluated in advance. Qian et al.²² suggested that g could be expressed as the product of a concentration-dependent term and a temperature-dependent term for binary liquid-liquid phase diagrams. In this study the experimentally measured χ values are represented by the following expression:

$$\chi = (a + b\phi_2)(1 + cT + dT^2) \quad (9)$$

where a , b , c , and d are parameters that can be estimated by a nonlinear regression method. Good fits of χ data were obtained using eq. (9), as shown in Figure 7. Once all the parameters are determined, the function of g is obtained directly from eq. (8).

Figure 8 illustrates the temperature dependency of g at four different volume fractions. Although χ assumes negative values, the values of g are positive and decrease monotonically with temperature and concentration. The positive values of g are caused by the strong concentration dependency of χ , which gives rise to a considerably high value of the second term containing the derivative of g with respect to ϕ_2 on the

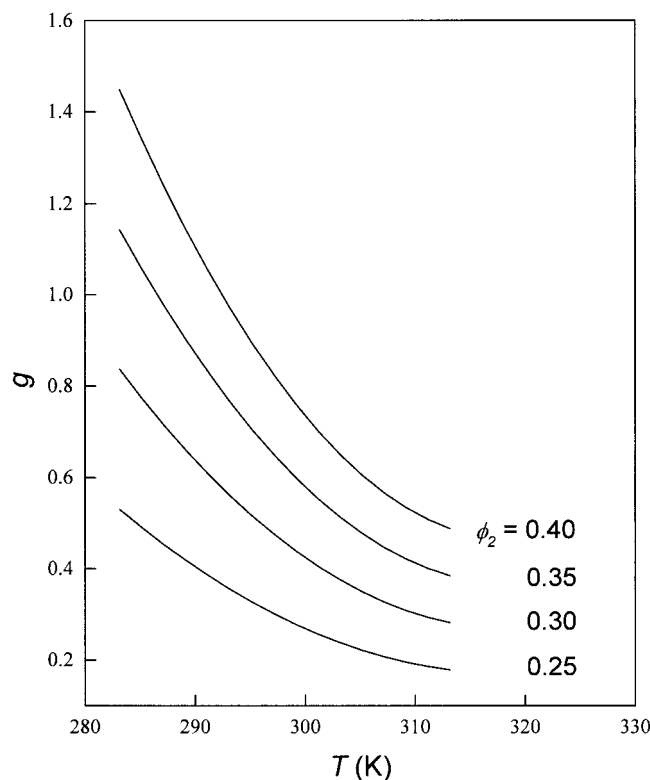


Figure 8 Effect of polymer volume fraction on the g parameter calculated using eq. (8) against temperature.

right-hand side in eq. (8). Similar to the interpretation of the χ parameter, large positive g (in this case, at low temperatures and high polymer concentrations) implies poor thermodynamic conditions, where the segments of polymer chains are preferentially attached together rather than being in contact with solvents. However, this association of polymer segments does not result in the formation of large crystallites, as evidenced by the fact that the corresponding gels did not show characteristic crystallization peaks in differential scanning calorimetry (DSC) experiments and birefringence under the polarized microscope. In contrast to the χ parameter, the plot based on the integral interaction parameter demonstrates that the association of polymer segments exists preferentially at low temperatures and high polymer concentrations, which is consistent with the gelation behavior in Figure 1, in that gelation occurs when lowering the temperature and high gel stability is achieved for high polymer concentrations.

The integral interaction parameter can be split into enthalpy (g_H) and entropy (g_S) contributions according to

$$g_H = -T \left(\frac{\partial g}{\partial T} \right) = \frac{\Delta H}{RTx_1\phi_2} \quad (10)$$

and

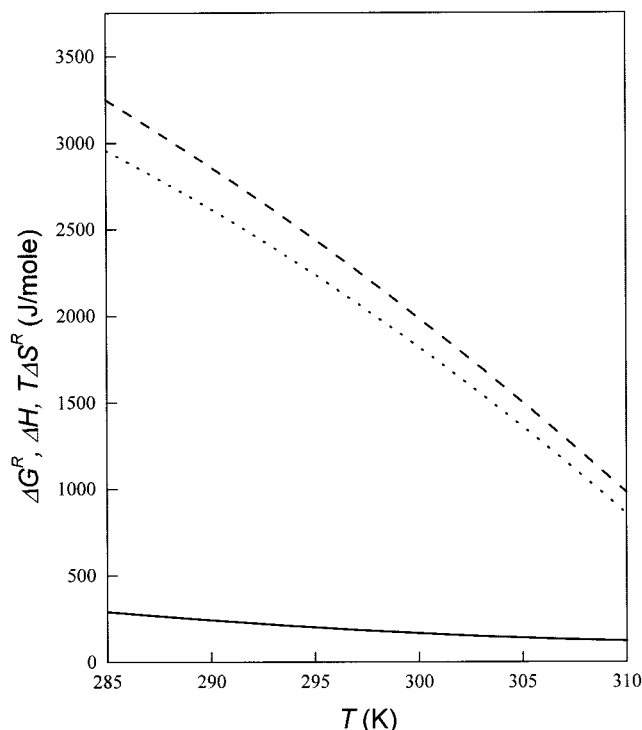


Figure 9 ΔG^R , ΔH , and $T\Delta S^R$ as a function of temperature (solid line: ΔG^R ; dashed line: ΔH ; dotted line: $T\Delta S^R$).

$$g_s = g - g_H = - \frac{\Delta S^R}{R x_1 \phi_2} \quad (11)$$

where ΔH and ΔS^R are the molar enthalpy of mixing and the residual molar entropy of mixing, respectively. We plot the variation of ΔG^R , ΔH , and $T\Delta S^R$ as a function of temperature in Figure 9 at a fixed ϕ_2 of 0.25. The enthalpy of mixing is positive and decreases with increasing temperature, indicating that energies required to exchange solvent molecules and polymer segments become higher at low temperatures. As a result of the large enthalpies of mixing at low temperatures, the association of polymer segments is energetically preferred. Nunes and Wolf²³ analyzed the integral interaction parameters of poly(*n*-butyl methacrylate) (PBMA) gels, which also exhibit positive ΔH , and they explained the thermoreversible gelation in terms of the formation of amorphous aggregates resulting from energetically favorable contacts between polymer segments. Our values of ΔH are of the same order of magnitude as those for PBMA gels. Hence, we expect that the association of polymer segments should be one of the contributors to the junctions of the gel network in nitrocellulose gels. Furthermore, the residual entropy of mixing is also positive, reflecting the increase in the degree of disorder resulting from the rupture of segment contacts.

The interpretation of the temperature and concentration dependencies of the integral interaction pa-

rameters is similar to that for the linear relationship between T_m and $(\delta_p - \delta_s)^2$, which states that the stability of a gel is directly associated with the enthalpy of mixing resulting from the difficulty in breaking the intersegmental contacts of adjacent polymers. Therefore, one can conclude that the strength of associating segments increases at low temperatures (large values of ΔH) or in poor solvents (large differences between solubility parameters).

CONCLUSIONS

Nitrocellulose was demonstrated to form thermo-reversible gels in a variety of solvents. In particular, the gelation behavior and the thermodynamic properties of nitrocellulose in ethyl acetate were examined. At a low-concentration limit, the critical gel concentration is approximately proportional to the reciprocal of molecular weight, similar to the criterion that divides the viscosity behavior of polymer solutions according to the effect of entanglements. Second, the reduced critical gel concentrations $C_{gel}[\eta]$ lie at the regime of concentrated solutions, having values higher than those corresponding to the onset of entanglement effects in the master curve of a viscosity plot. These facts lead to the conclusion that the entanglement of polymer chains is a necessary condition for the formation of nitrocellulose gels.

The phase behavior of the sol-gel transition is analyzed using the Ferry and Eldridge relations, and the low values of the gelation enthalpy are consistent with the view that the formation of networks is primarily attributed to entanglements. However, the average number of polymer chains in a junction point is larger than two ($n = 2$ in the case of entanglements), especially for low molecular weight samples, indicating that factors other than entanglements also contribute to the junction points of networks.

A possible explanation for the values of n is that, in addition to entanglements, the association of polymer segments may also stabilize the network junctions. The thermodynamic analysis based on the solubility parameters and the integral interaction parameters confirms that the association of polymer segments exists under poor thermodynamic conditions (at low temperatures or in poor solvents). The plot of T_m against $(\delta_p - \delta_s)^2$ for a variety of solvents shows that the gel stability is enhanced by a poor solvent, where polymer chains are preferentially in contact with each other. Similarly, the positive values of g and the increase of g with decreasing temperature, together with the extraordinarily high values of the enthalpy of mixing at low temperatures, indicate that the association of polymer segments is favored at low temperatures.

This work was supported by the National Science Council of the Republic of China through the project NSC 89-2216-E-218-003.

References

1. te Nijenhuis, K. *Thermoreversible Networks*; Springer-Verlag: Berlin, 1997.
2. Boyer, R. F.; Baer, E.; Hiltner, A. *Macromolecules* 1985, 18, 427.
3. Yang, Y. C.; Geil, P. H. *J Macromol Sci Phys* 1983, B22, 463.
4. Newman, S.; Krigbaum, W. R.; Carpenter, D. K. *J Phys Chem* 1956, 60, 648.
5. Doolittle, A. K. *Ind Eng Chem* 1946, 38, 535.
6. Viney, C.; Windle, A. H. *J Mater Sci Lett* 1986, 5, 516.
7. Vrancken, M. N.; Ferry, J. D. *J Polym Sci* 1957, 14, 27.
8. Holt, C.; Mackie, W.; Sellen, D. B. *Polymer* 1976, 17, 1027.
9. Schurz, J.; Tritthart, H. *Polymer* 1966, 7, 475.
10. Ninomiya, K.; Ferry, J. D. *J Polym Sci A2* 1964, 5, 195.
11. Orts, W. J.; Godbout, L.; Marchessault, R. H.; Revol, J. F. *Macromolecules* 1998, 31, 5717.
12. Kamada, K.; Sato, H. *Polym J* 1971, 2, 489.
13. Nunes, S. P.; Wolf, B. A.; Jeberien, H. E. *Macromolecules* 1987, 20, 1948.
14. Graessley, W. W. *Polymer* 1980, 21, 258.
15. Castelain, C.; Doublier, J. L.; Lefebvre, J. *Carbohydr Polym* 1987, 7, 1.
16. Launay, B.; Cuvelier, G.; Martinez-Reyes, S. *Carbohydr Polym* 1997, 34, 385.
17. Quinchon, J.; Tranchant, J. *Nitrocellulose*; Ellis Horwood: Chichester, UK, 1989.
18. Eldridge, J. E.; Ferry, J. D. *J Phys Chem* 1954, 58, 992.
19. Tan, H. M.; Moet, A.; Hiltner, A.; Baer, E. *Macromolecules* 1983, 16, 28.
20. Watase, M.; Nishinari, K. *Polym J* 1986, 18, 1017.
21. Gundert, F.; Wolf, B. A. *Polymer Handbook: Polymer-Solvent Interaction Parameters*; Wiley: New York, 1989.
22. Qian, C.; Mumby, S. J.; Eichinger, B. E. *Macromolecules* 1991, 24, 1655.
23. Nunes, S. P.; Wolf, B. A. *Macromolecules* 1987, 20, 1952.